Curr Radiol Rep (2014) 2:74
DOI 10.1007/s40134-014-0074-8

Recent Developments in Multiparametric Prostate MR Imaging

Rajan T. Gupta · Thomas J. Polascik · Samir S. Taneja · Andrew B. Rosenkrantz

Published online: 14 October 2014

Abstract Multiparametric magnetic resonance imaging (mpMRI) of the prostate has become a mature and accepted technology in the evaluation of the patient with suspected prostate cancer (PCa). This review focuses on key recent developments in the area of mpMRI, specifically: reporting systems used by radiologists when interpreting mpMRI, advances in technical aspects of diffusion-weighted imaging (DWI), and innovations in MRI-ultrasound (MRI-US) fusion-guided prostate biopsies. These topics were selected given that reporting systems are critical when communicating findings on mpMRI of the prostate to referring clinicians, advanced techniques in DWI have improved the detection and characterization of PCa, and MRI-US fusion biopsies now enable more accurate targeting of suspicious lesions at biopsy, including lesions that are difficult to visualize using standard B-mode ultrasound imaging. Radiologists interpreting prostate MRI today are likely to incorporate aspects of all three of these topics into their current practice.

Keywords Prostate cancer · Multiparametric prostate MRI · Diffusion-weighted imaging · MRI-ultrasound fusion biopsy

This article is part of the Topical Collection on *Urogenital Imaging*.

R. T. Gupta (✉)
Department of Radiology, Duke University Medical Center (DUMC), Box 3808, Durham, NC 27710, USA
e-mail: rajan.gupta@duke.edu

T. J. Polascik
Division of Urologic Surgery and Duke Prostate Center, Department of Surgery, Duke University Medical Center (DUMC), Box 2804, Durham, NC 27710, USA

S. S. Taneja
Division of Urologic Oncology, Department of Urology, New York University Langone Medical Center, 550 First Avenue, New York, NY 10016, USA

A. B. Rosenkrantz
Department of Radiology, New York University Langone Medical Center, 550 First Avenue, New York, NY 10016, USA

Introduction

Multiparametric magnetic resonance imaging (mpMRI) of the prostate has become a mature and accepted technology in the evaluation of the patient with suspected prostate cancer (PCa). This technology facilitates more accurate lesion localization, particularly for anterior tumors that are commonly missed on systematic transrectal ultrasound-guided (TRUS-guided) biopsy. While the use of MRI to evaluate the prostate dates back over three decades [1], its more recent evolution to multiparametric evaluation of the prostate now offers a wealth of functional information that enables vastly improved detection and characterization of PCa. Previously, in comparison, MRI of the prostate, due to its reliance on lesion morphology and signal changes on conventional T1-weighted imaging and T2-weighted imaging (T2WI), suffered from relatively poor sensitivity and specificity for detecting PCa.

It is generally accepted that two functional sequences in addition to anatomic T2WI constitute a mpMRI of the prostate [2••]. The functional sequences in current practice include diffusion-weighted imaging (DWI), dynamic contrast-enhanced MRI (DCE-MRI), and MR spectroscopic imaging (MRSI). While DWI, among these, has become established as an essential sequence in mpMRI protocols, research has shown that any two functional sequences in addition to T2WI yield substantially better results for

diagnosis of PCa compared with one functional sequence alone. In this review, we focus on three recent and ongoing developments in the area of mpMRI of the prostate, specifically: structured reporting of this modality, advanced techniques in DWI, and MRI-US fusion biopsies.

Multiparametric MRI Reporting

Due to the volume of functional information now made available by mpMRI, it can be difficult to synthesize this information into a usable report for the referring clinician. In addition, each sequence within the mpMRI protocol has its own strengths and weaknesses. For example, T2WI, reflecting tissue water content, is considered to be the best sequence for anatomic delineation of the prostate, including its margins and zonal anatomy, although focal abnormalities on this sequence are caused by a wide range of pathologies and are non-specific for tumor. DWI reflects tissue cellularity and has been shown in numerous studies to improve lesion localization and characterization, in particular reflecting lesion aggressiveness as determined by the histopathologic Gleason scoring system [3–9]. Moreover, DCE-MRI, reflecting tissue vascularity, may assist the radiologist in interpretation of challenging cases or direct the radiologist to identify lesions not apparent using the other techniques, thereby providing a further incremental improvement in accuracy in the detection of PCa [10, 11]. Given the need to integrate typically variable findings from these sequences, standardized interpretation and reporting schemes have been proposed for prostate mpMRI, similar to those used in breast imaging and liver imaging. Ideally, such systems will allow for reproducible and standardized reports, thus limiting subjectivity in the interpretation of mpMRI and possibly enabling broader and more consistent adoption of the technique [12•].

One such proposed system was detailed in a report from a European Society of Urogenital Radiology (ESUR) expert panel in 2012, entitled Prostate Imaging and Reporting Archiving Data System (PI-RADS) [2••]. PI-RADS is perhaps the most widely recognized formal prostate interpretation system and provides structured criteria for assigning each detected lesion a score from 1 to 5 for each sequence that comprises the mpMRI (T2WI, DWI, DCE-MRI, and, if available, MRSI). This score is intended to reflect the likelihood that clinically significant disease is present, with 1 representing the lowest likelihood and 5 representing the highest likelihood. Also, given that different sequences have different values in lesion detection and characterization depending on location and other considerations, a separate composite score from 1 to 5 is also assigned, reflecting the overall likelihood that the lesion reflects a clinically significant cancer [12•]. While there are varying perspectives regarding how best to derive this overall score, it is suggested that this score not simply be a "sum" or "average" of the individual sequence scores, which fails to reflect the variable importance of each sequence in a given context. Rather, based on a new consensus between the ESUR prostate MRI working group as well as the PI-RADS steering committee of the American College of Radiology (ACR) [12], it is currently advised that the overall score be weighted to reflect the "dominant" sequence parameter. The "dominant" sequence parameter is DWI for lesions in the peripheral zone, T2WI for lesions in the transition zone, and DCE-MRI when detecting PCa recurrence [12•] (Fig. 1).

Recent work has attempted to compare the performance of PI-RADS scoring against a Likert scale in determining the likelihood of clinically significant tumor in the prostate [13]. A Likert scheme uses the overall impression of the radiologist, without application of fixed criteria or individual assessments for each sequence, to generate a score on a 1–5 scale, whereas PI-RADS uses explicit criteria for each sequence and in generation of the overall score [13]. One recent study observed that interreader reproducibility tended to be higher for more experienced readers (4–6 years of post-fellowship training experience with prostate mpMRI in this study) than for less experienced readers (0–1 year of post-fellowship training) as well as higher in the PZ than in the TZ [13]. For the subset of more experienced readers, reproducibility was similar for PI-RADS and the Likert scale in the PZ, but interestingly was somewhat higher for the Likert scale than for PI-RADS in the TZ [13]. It should be noted that, although this study was performed prior to the consensus agreement on the overall PI-RADS score between the ESUR prostate MRI expert working group and the ACR steering committee for PI-RADS [12•], the findings nonetheless underscore the importance of standardized reporting for prostate mpMRI interpretation, regardless of which specific system is used. The consensus agreement between these two groups will likely be an important step in the right direction given that it is the overall score that ultimately is most relevant in the characterization of clinically significant PCa and for which high reproducibility is therefore essential.

Advances in Diffusion-Weighted Imaging

DWI has become established as an essential sequence within multiparametric prostate MRI protocols, being included among a list of "minimal" technical requirements in the ESUR consensus guidelines published in 2012 [2••]. Numerous studies confirm the value of DWI in improving tumor detection and localization [4, 14, 15]. DWI also contributes to assessment of tumor volume [16], risk stratification in active surveillance candidates [17], and prediction of biochemical recurrence [18]. In addition, one study observed that a "biparameter" protocol incorporating

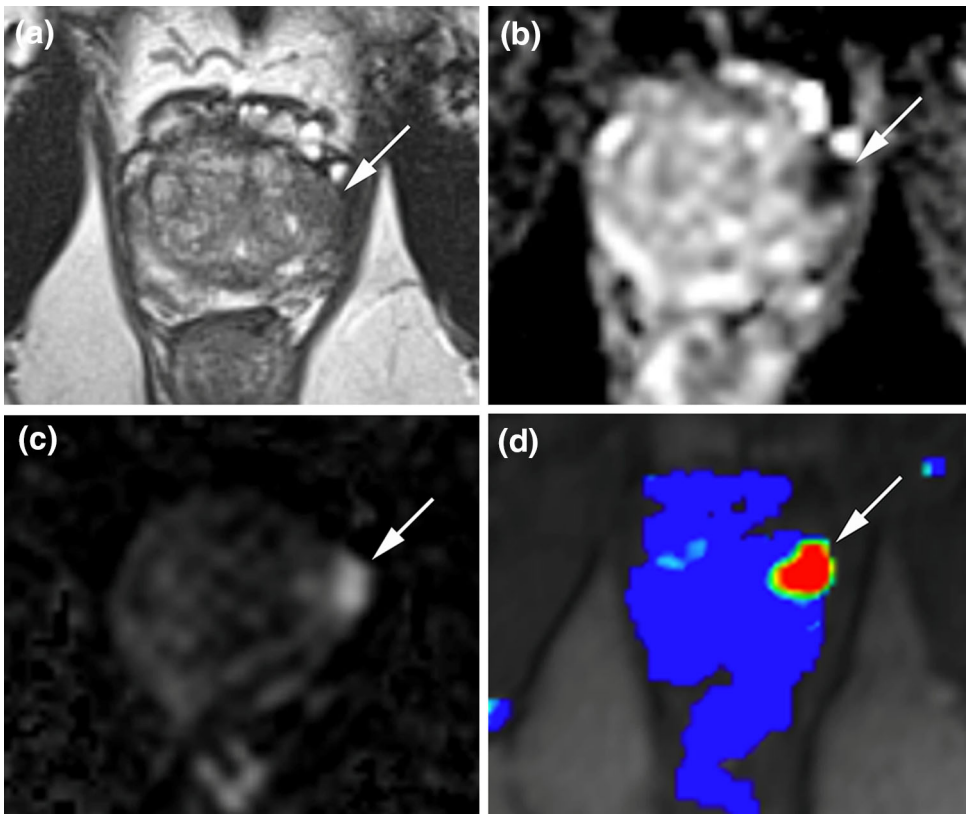

Fig. 1 A 72-year-old male was referred for multiparametric prostate MRI (mpMRI). **a** Axial T2W image shows a mass-like area of decreased T2 signal intensity within the left anterolateral peripheral zone (*white arrow*). **b** Axial ADC map shows corresponding area of substantially low ADC, suggesting a higher-grade tumor (*white arrow*). **c** Calculated diffusion-weighted image at *b*-value of 1,500 s/mm^2 shows this area to have increased signal (*white arrow*). **d** Colorized washout map created using post-processing software from dynamic contrast-enhanced MRI (DCE-MRI) acquisition shows this area to have abnormal perfusion kinetics (*white arrow*). Given that this lesion is in the peripheral zone, the "dominant" parameter for determining the overall PI-RADS score is the score obtained from DWI/ADC. In this patient, the DWI/ADC score, and thus the overall PI-RADS score, are both 5/5. This lesion corresponded with a Gleason 7 tumor at targeted biopsy (Color figure online)

solely T2WI and DWI had strong performance in tumor detection in men without prior prostate biopsy [19]. Recent studies explore strategies for the optimization of the acquisition, post-processing, and interpretation of DWI; such considerations are important to achieve maximal diagnostic benefit from this key sequence.

One principle aspect of DWI acquisition is selection of the sequence's maximal *b*-value. The *b*-value refers to the strength of diffusion-sensitizing gradients that are applied during the sequence and generate image contrast that reflects the tissue behavior of water molecule. The ESUR guidelines suggest use of a maximal *b*-value of approximately 1,000 s/m^2 [2••], which indeed has been used in earlier studies with reasonable success [15, 20]. A challenge in use of this *b*-value is that benign prostate tissue often continues to demonstrate mild increased signal, which can limit optimal visualization of tumor. More recently, use of even higher *b*-values in the range of 1,500–2,000 s/mm^2 has gained interest. Such ultra high *b*-values are higher than those typically used in other organs, although they may have value when used in the prostate. At these higher *b*-values, there is increased suppression of signal within benign prostate tissue, which in turn can provide improved conspicuity of focal lesions and hence better tumor detection (Fig. 2). As of now, at least six studies have compared tumor detection between *b*-1,000 and *b*-2,000 images and report improved accuracy using the *b*-2,000 images [21–26]. For instance, in one study, two readers of varying experience using solely the high *b*-value images for tumor detection achieved significantly higher sensitivity on the *b*-2,000 than on the *b*-1,000 images (86.2 vs. 51.7 % and 69.0 vs. 24.1 %, respectively) without a significant loss in positive predictive value [24]. Furthermore, the improved performance using a *b*-value of 2,000 s/mm^2 has been observed in both the peripheral zone and the transition zone [26]. Thus, radiologists should consider routinely incorporating *b*-2,000 images into their institutional protocol.

While ultra high *b*-values have the potential to improve diagnostic performance of prostate DWI, acquisition of such images can be technically challenging due to

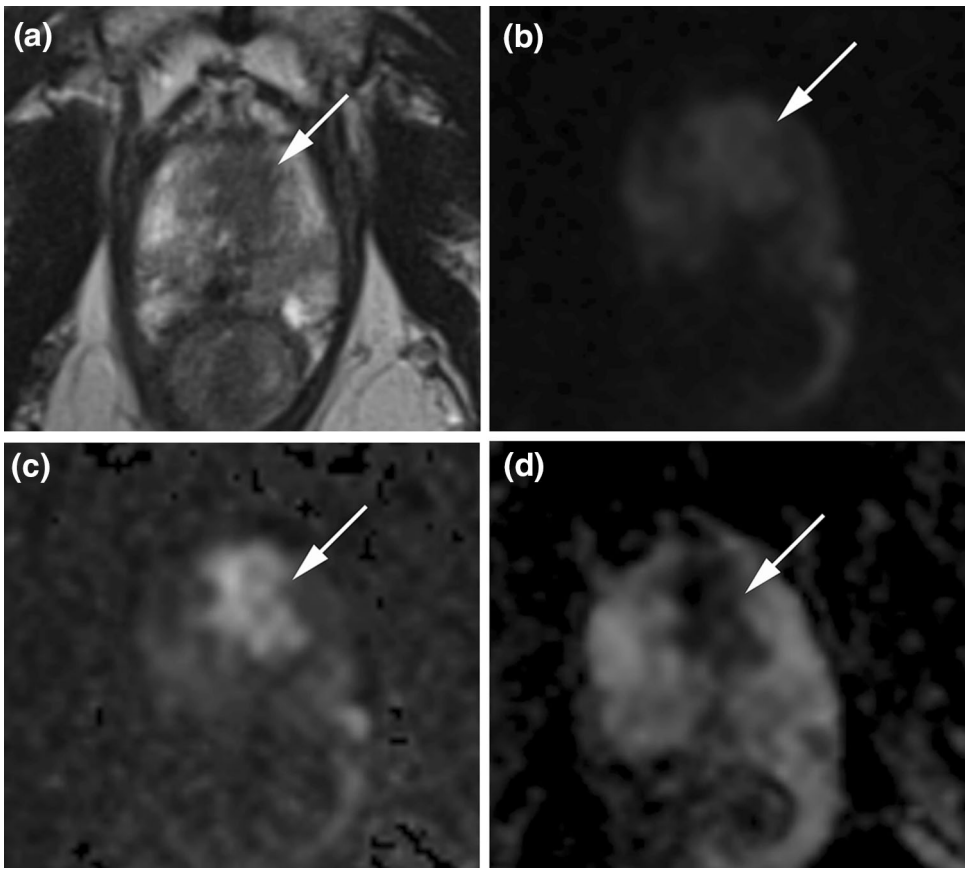

Fig. 2 A 74-year-old male was referred for multiparametric prostate MRI (mpMRI). **a** Axial T2W image shows a mass-like area of decreased T2 signal intensity within the anterior transition zone (*white arrow*). **b** Diffusion-weighted image acquired at *b*-value of 1,000 s/mm^2 reveals this area to have increased signal (*white arrow*). **c** Calculated diffusion-weighted image at *b*-value of 1,500 s/mm^2 shows this area (*white arrow*) to be even more conspicuous than on the acquired DWI at *b*-value of 1,000 s/mm^2. **d** Axial ADC map shows corresponding low ADC (*white arrow*). This lesion corresponded with a Gleason 6 tumor at targeted biopsy

decreased signal-to-noise ratio and increased image distortion and susceptibility artifact encountered with increasing *b*-values. The extent of such challenges can depend on the particular scanner vendor and model, receiver coil, and software available for image acquisition. A recently proposed method for addressing the potential technical challenges of ultra high *b*-value imaging is to, rather than directly acquire such images, extrapolate instead the images from routine lower *b*-values [27]. That is, a mono-exponential fit can be applied to images obtained using *b*-values up to 1,000 s/mm^2 to calculate the expected signal intensity at the higher *b*-value and thereby derive the higher *b*-value image set. This technique, achieved via post-processing, eliminates the need to be able to directly acquire ultra high *b*-value images and also requires no additional scan time beyond the acquisition of standard *b*-value images. The computed ultra high *b*-value images achieve the very strong diffuse contrast provided by direct ultra high *b*-value images, although avoid the associated distortions and other artifacts. Three studies of computed *b*-values in the range of 1,400–1,500 s/mm^2 not only all report improved performance compared with acquired *b*-1,000 images [28–30], but also further suggest possible improvements in image quality or diagnosis compared with the directly acquired ultra high *b*-values [29, 30].

An additional important role of DWI is for assessment of PCa aggressiveness. Specifically, the apparent diffusion coefficient (ADC) of PCa is inversely proportional to tumor cellularity [31] as well as the Gleason score of PCa [32–34]. Given this relationship, ADC values have been applied to predict more reliably the Gleason score obtained from pathologic assessment of prostatectomy specimens than that predicted by the biopsy-based Gleason score [35•]. Thus, there is clearly a potentially large role to use the ADC value as a clinical biomarker in PCa management. However, the ability to implement the same successfully in individual patients has been limited by interpatient variation in the ADC values of normal benign peripheral zone as well as by overlap in the ADC values of tumors of different Gleason scores [36].

Given such challenges, attention has recently been given to the optimization of strategies for reliably predicting Gleason score based on diffusion metrics. One straightforward approach has been to perform an intrasubject normalization by computing the ratio between the ADC value of tumor and normal peripheral zone within a given subject [36]. Two studies have demonstrated significantly improved performance for predicting PCa aggressiveness using such normalized ADC values compared to using non-normalized data [36, 37]; for instance, one study reported

an improvement in the area-under-the-curve for identifying tumor with a Gleason score of 8 or 9, from 0.77 to 0.90 [36].

An additional technique that has been applied to improve the assessment of tumor aggressiveness using DWI is to apply a whole-lesion histogram analysis to the ADC measurements. That is, rather than obtaining ADC measurements using a single region-of-interest placed on only a portion of the tumor on a single slice, histogram measures can be obtained from 3D ROIs encompassing the entire tumor on all slices; such whole-lesion metrics not only more comprehensively sample the entire lesion, but also can provide measures of lesion texture and heterogeneity on DWI [38]. In one study, the ADC entropy obtained from whole-lesion histogram analysis outperformed standard mean ADC in characterizing the Gleason 4 component in Gleason 7 PCa for two independent readers [38]. In another study, the 10th percentile ADC from whole-lesion analysis showed the strongest correlation with Gleason score among various ADC parameters, including both mean and median ADC [39].

One further approach being explored to improve estimation of tumor aggressiveness using DWI is to apply more advanced models to the analysis of raw diffusion data in order to generate more sophisticated metrics than the ADC value obtained from a standard mono-exponential fit. It is hoped that these more novel metrics will better reflect the structural heterogeneity of PCa and show less overlap between tumors of different Gleason scores. Of note, the diffusion kurtosis model uses ultra high *b*-values of approximately 2,000 s/mm^2 to estimate the non-Gaussianity of diffusion behavior, reflecting microstructural complexity of tissue [40]. In one study, the kurtosis coefficient showed improvement in performance compared with ADC in differentiating benign and malignant prostate tissue [41]. In another study, the kurtosis of prostate tumors achieve significantly improved performance compared with ADC in predicting a Gleason score of 7 or greater (areas-under-the-curve of 0.70 vs. 0.62, respectively) [42]. Nonetheless, the additive value of the diffusion kurtosis model has not been confirmed in all studies [43], and as such, the role of this technique remains preliminary, and further investigation is required.

MRI-Ultrasound Fusion Biopsies

TRUS-guided biopsies have long been the standard of care for diagnosis in men with suspected PCa. However, there is recognition of substantial sampling error intrinsic in systematic TRUS-guided biopsy [44–46], which leads to undergrading of disease in up to 46 % of patients [47–49]. This undergrading can potentially contribute to suboptimal selection of a therapeutic strategy in some patients. An alternative to TRUS-guided biopsy is the 3D transperineal mapping biopsies (TPMB); although still "random," this technique is intended to provide more complete sampling of the gland [50]. Nonetheless, TPMB remains subject to sampling error (albeit to a lesser extent), often requires performance in the operating room under general anesthesia, and conveys a higher complication rate than TRUS-guided biopsy due to the substantially increased number of biopsy samples [50].

In light of the above challenge, attention has shifted to targeted biopsies using information gleaned from mpMRI. Targeted prostate biopsy may be performed using a "cognitive" approach that does not entail any specialized equipment in which the operator initially views the MRI and then uses ultrasound guidance to take additional cores from the suspicious area without direct visualization of the MRI lesion; although this is relatively easy to implement in clinical practice and has shown reasonable results [51•], this approach does not achieve optimal lesion targeting. Two methods using advanced technology to improve lesion targeting are direct in-bore MRI-guided biopsy [52] and MRI-US software fusion biopsy [53]. We believe that MRI-US fusion biopsy will be the trend of the future in PCa diagnosis given its relative ease, efficiency, and patient comfort, as well as its ability to readily sample multiple lesions and potentially perform systematic sampling of the prostate, all within a single session. Indeed, there is a surge of interest in MRI-US fusion biopsy among urologists, and this technique is being supported by a rapidly growing body of literature [54–58]. Therefore, in this section, we focus further on MRI-US fusion biopsy. Fusion systems allow previously obtained mpMRI images to be "fused" and "overlaid" real-time to guide TRUS-guided biopsies in the outpatient setting [53, 54, 59] (Fig. 3). While we anticipate that fusion systems will eventually become used even for initial prostate biopsies, such systems currently have particular value in the patient who has persistent suspicion for PCa following previous negative TRUS-guided biopsies; fusion biopsy has been shown to detect cancer in up to 40 % of these patients [60•]. Perhaps even more importantly, approximately 33 % of these men were diagnosed with Gleason 8 cancer or higher [61]. It is believed that improved detection of clinically significant cancer, and decreased detection of insignificant cancer, can be facilitated by mpMRI with MRI-US fusion biopsy of suspicious lesions [53], which is particularly important given increasing concerns within the lay and medical communities regarding PCa "overdiagnosis" and "overtreatment".

Several vendors currently offer commercial MRI-US fusion biopsy systems, each having its own strengths and weaknesses. In general, implementation of such systems

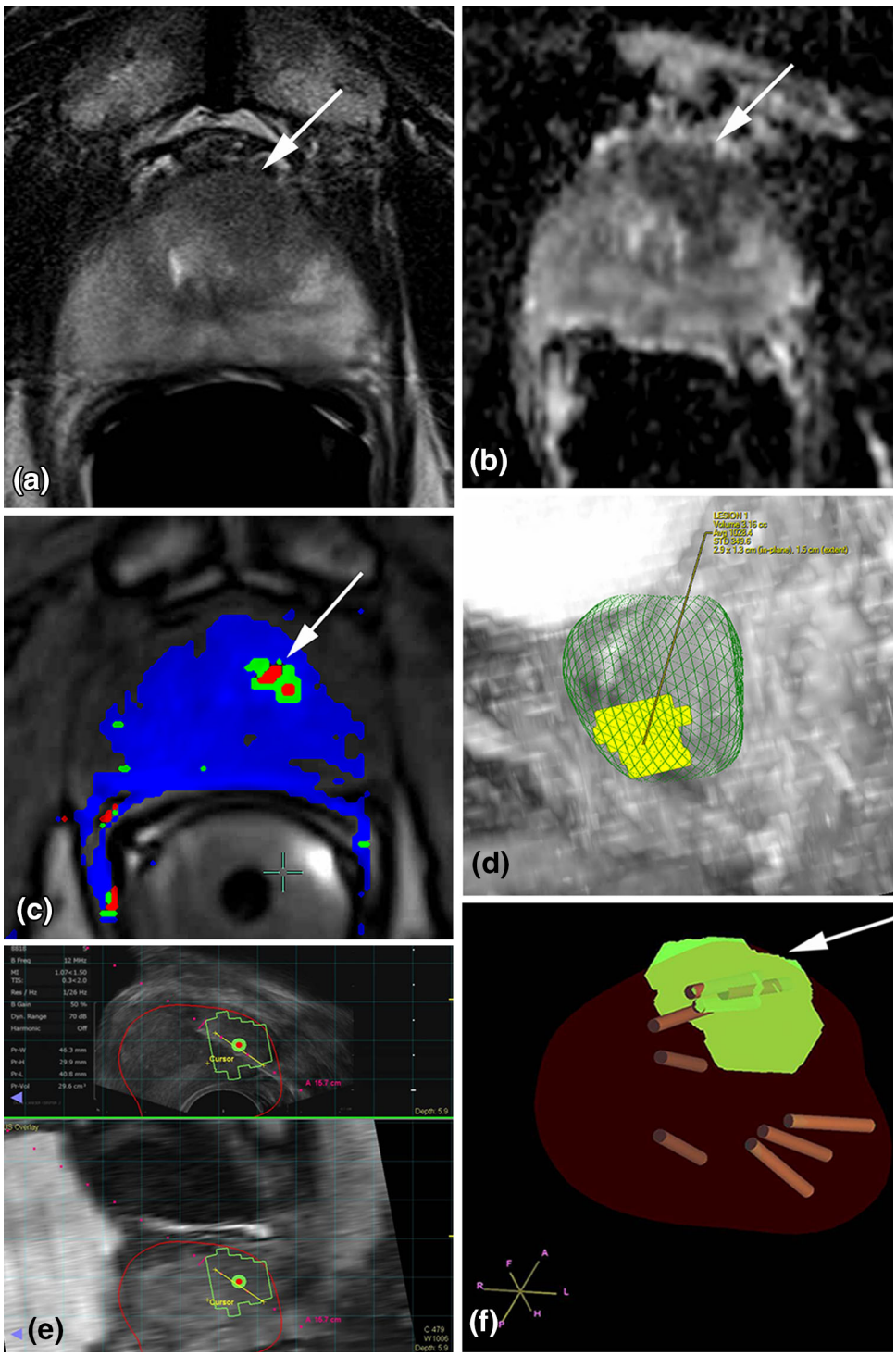

Fig. 3 A 66-year-old male with PSA of 9.7 ng/mL and no prior prostate biopsies was referred for multiparametric prostate MRI. **a** Axial T2W image shows a large poorly marginated mass-like area of homogeneous decreased T2 signal intensity within the left anterior transition zone (*white arrow*). **b** Axial ADC map shows corresponding moderately reduced ADC (*white arrow*). **c** Colorized perfusion map created using post-processing software from dynamic contrast-enhanced MRI (DCE-MRI) acquisition shows corresponding abnormal perfusion (*white arrow*). This lesion is highly suspicious for a transition zone tumor. **d** Maximal intensity projection (MIP) of the lesion (*yellow*) and the prostate gland boundary (*green*) are shown for pre-biopsy planning prior to MRI-US fusion biopsy. **e** Images obtained during MRI-US fusion biopsy of this lesion (*outlined in green*) with needle passage through the area of interest using UroNav system (InVivo Corp., Gainesville, FL, USA). **f** Additional post-biopsy 3D reconstruction images showing the needle tracts through the lesion (*yellow*) as well as other systematic biopsy tracts (*orange*). MRI-US fusion-targeted biopsy of this lesion confirmed the presence of a Gleason $5 + 4 = 9$ transition zone tumor in this location (Color figure online)

entails an initial planning phase prior to the biopsy session in which the prostate boundary and target lesions are annotated on the MR images, a full ultrasound scan of the prostate at the start of the biopsy session to allow for mapping to the segmented MR images, and subsequent biopsy based on a tracking mechanism to guide the operator to the predefined targets [62, 63]. Tracking mechanisms employed in current clinical practice include mechanical navigation via a robotic arm to which the ultrasound probe is attached, as well as external mechanical field navigation in which sensors are inserted into the ultrasound probe that is under freehand control by the operator [62, 63]. Data suggest that the fusion system is of most value relative to cognitive targeting for lesions that

are most difficult to reliably access via cognitive targeting, such as a lesion that is anterior in location or small in size [64]. Thus, critical to the success of these systems is achieving accurate fusion of the mpMRI images to the real-time TRUS images. Although simulations suggest that a registration accuracy of 1.9 mm is required to correctly grade 95 % of lesions via fusion biopsy [65], current fusions systems have been suggested to have a root mean squared error of 3.5 mm [66]. Therefore, improved accuracy of coregistration is an important component of continued optimization of fusion systems. Other areas for future development include improved compensation for patient motion and improved workflow to foster clinical acceptance. This could include more efficient automated and semi-automated algorithms for prostate segmentation prior to the biopsy session and a more efficient procedure, with less operator interaction, for achieving MRI-US registration following the ultrasound scan at the start of the biopsy session.

Conclusion

As the utilization of multiparametric prostate MRI expands, continued focus will be on the ability of radiologists to reproducibly report results, the development of cutting-edge techniques for lesion detection and characterization, and finally, the refinement of a biopsy system that allows for accurate and complete sampling of the index lesion and any other clinically significant tumors. For these reasons, this review has focused on the current knowledge on prostate mpMRI reporting, advances in DWI, and MRI-US fusion biopsies.

Compliance with Ethics Guidelines

Conflict of Interest Dr. Rajan T. Gupta, Dr. Thomas J. Polascik, Dr. Samir S. Taneja, and Dr. Andrew B. Rosenkrantz each declare no potential conflicts of interest.

Human and Animal Rights and Informed Consent This article does not contain any studies with human or animal subjects performed by any of the authors.

References

Papers of particular interest, published recently, have been highlighted as:
- • Of importance,
- •• Of major importance

1. Steyn JH, Smith FW. Nuclear magnetic resonance imaging of the prostate. Br J Urol. 1982;54(6):726–8.
2. •• Barentsz JO, Richenberg J, Clements R, Choyke P, Verma S, Villeirs G et al. ESUR prostate MR guidelines 2012. Eur Radiol. 2012;22(4):746–57. *This report represents the work of the ESUR expert panel in formulating guidelines for the performance and interpretation of multi-parametric prostate MRI. The article is of particular importance given that it provides the initial presentation of the PI-RADS system for structured reporting of prostate MRI.*
3. Delongchamps NB, Beuvon F, Eiss D, Flam T, Muradyan N, Zerbib M, et al. Multiparametric MRI is helpful to predict tumor focality, stage, and size in patients diagnosed with unilateral low-risk prostate cancer. Prostate Cancer Prostatic Dis. 2011;14(3):232–7.
4. Tamada T, Sone T, Higashi H, Jo Y, Yamamoto A, Kanki A, et al. Prostate cancer detection in patients with total serum prostate-specific antigen levels of 4–10 ng/mL: diagnostic efficacy of diffusion-weighted imaging, dynamic contrast-enhanced MRI, and T2-weighted imaging. AJR Am J Roentgenol. 2011;197(3):664–70.
5. Isebaert S, Van den Bergh L, Haustermans K, Joniau S, Lerut E, De Wever L, et al. Multiparametric MRI for prostate cancer localization in correlation to whole-mount histopathology. J Magn Reson Imaging. 2013;37(6):1392–401.
6. Chen M, Dang HD, Wang JY, Zhou C, Li SY, Wang WC, et al. Prostate cancer detection: comparison of T2-weighted imaging, diffusion-weighted imaging, proton magnetic resonance spectroscopic imaging, and the three techniques combined. Acta Radiol. 2008;49(5):602–10.
7. Tan CH, Wei W, Johnson V, Kundra V. Diffusion-weighted MRI in the detection of prostate cancer: meta-analysis. AJR Am J Roentgenol. 2012;199(4):822–9.
8. Wu LM, Xu JR, Ye YQ, Lu Q, Hu JN. The clinical value of diffusion-weighted imaging in combination with T2-weighted imaging in diagnosing prostate carcinoma: a systematic review and meta-analysis. AJR Am J Roentgenol. 2012;199(1):103–10.
9. Delongchamps NB, Rouanne M, Flam T, Beuvon F, Liberatore M, Zerbib M, et al. Multiparametric magnetic resonance imaging for the detection and localization of prostate cancer: combination of T2-weighted, dynamic contrast-enhanced and diffusion-weighted imaging. BJU Int. 2011;107(9):1411–8.
10. Girouin N, Mege-Lechevallier F, Tonina Senes A, Bissery A, Rabilloud M, Marechal JM. Prostate dynamic contrast-enhanced MRI with simple visual diagnostic criteria: is it reasonable? Eur Radiol. 2007;17(6):1498–509.
11. Tanimoto A, Nakashima J, Kohno H, Shinmoto H, Kuribayashi S. Prostate cancer screening: the clinical value of diffusion-weighted imaging and dynamic MR imaging in combination with T2-weighted imaging. J Magn Reson Imaging. 2007;25(1):146–52.
12. • Bomers JG, Barentsz JO. Standardization of multiparametric prostate MR imaging using PI-RADS. Biomed Res Int. 2014. doi:10.1155/2014/431680. *This article provides a summary of how the PI-RADS system for structured reporting of prostate MRI may be performed in clinical practice. Specific case examples are presented, and the concept of use of the "dominant" sequence score for determining the "overall" PI-RADS score is demonsrated.*
13. Rosenkrantz AB, Lim RP, Haghighi M, Somberg MB, Babb JS, Taneja SS. Comparison of interreader reproducibility of the prostate imaging reporting and data system and likert scales for evaluation of multiparametric prostate MRI. AJR Am J Roentgenol. 2013;201(4):W612–8.
14. Haider MA, van der Kwast TH, Tanguay J, Evans AJ, Hashmi AT, Lockwood G, et al. Combined T2-weighted and diffusion-weighted MRI for localization of prostate cancer. AJR Am J Roentgenol. 2007;189(2):323–8.

15. Lim HK, Kim JK, Kim KA, Cho KS. Prostate cancer: apparent diffusion coefficient map with T2-weighted images for detection—a multireader study. Radiology. 2009;250(1):145–51.
16. Mazaheri Y, Hricak H, Fine SW, Akin O, Shukla-Dave A, Ishill NM, et al. Prostate tumor volume measurement with combined T2-weighted imaging and diffusion-weighted MR: correlation with pathologic tumor volume. Radiology. 2009;252(2):449–57.
17. van As NJ, de Souza NM, Riches SF, Morgan VA, Sohaib SA, Dearnaley DP, et al. A study of diffusion-weighted magnetic resonance imaging in men with untreated localised prostate cancer on active surveillance. Eur Urol. 2009;56(6):981–7.
18. Park JJ, Kim CK, Park SY, Park BK, Lee HM, Cho SW. Prostate cancer: role of pretreatment multiparametric 3-T MRI in predicting biochemical recurrence after radical prostatectomy. AJR Am J Roentgenol. 2014;202(5):W459–65.
19. Rais-Bahrami S, Siddiqui MM, Vourganti S, Turkbey B, Rastinehad AR, Stamatakis L, et al. Diagnostic value of biparametric MRI as an adjunct to PSA-based detection of prostate cancer in men without prior biopsies. BJU Int. 2014. doi:10.1111/bju.12639.
20. Vilanova JC, Barcelo-Vidal C, Comet J, Boada M, Barcelo J, Ferrer J, et al. Usefulness of prebiopsy multifunctional and morphologic MRI combined with free-to-total prostate-specific antigen ratio in the detection of prostate cancer. AJR Am J Roentgenol. 2011;196(6):W715–22.
21. Tamada T, Kanomata N, Sone T, Jo Y, Miyaji Y, Higashi H, et al. High b value (2,000 s/mm^2) diffusion-weighted magnetic resonance imaging in prostate cancer at 3 Tesla: comparison with 1,000 s/mm^2 for tumor conspicuity and discrimination of aggressiveness. PLoS One. 2014;9(5):e96619.
22. Manenti G, Nezzo M, Chegai F, Vasili E, Bonanno E, Simonetti G. DWI of prostate cancer: optimal b-value in clinical practice. Prostate Cancer. 2014;2014:868269.
23. Ueno Y, Kitajima K, Sugimura K, Kawakami F, Miyake H, Obara M, et al. Ultra-high b-value diffusion-weighted MRI for the detection of prostate cancer with 3-T MRI. J Magn Reson Imaging. 2013;38(1):154–60.
24. Rosenkrantz AB, Hindman N, Lim RP, Das K, Babb JS, Mussi TC, et al. Diffusion-weighted imaging of the prostate: comparison of b1000 and b2000 image sets for index lesion detection. J Magn Reson Imaging. 2013;38(3):694–700.
25. Metens T, Miranda D, Absil J, Matos C. What is the optimal b value in diffusion-weighted MR imaging to depict prostate cancer at 3T? Eur Radiol. 2012;22(3):703–9.
26. Katahira K, Takahara T, Kwee TC, Oda S, Suzuki Y, Morishita S, et al. Ultra-high-b-value diffusion-weighted MR imaging for the detection of prostate cancer: evaluation in 201 cases with histopathological correlation. Eur Radiol. 2011;21(1):188–96.
27. Blackledge MD, Leach MO, Collins DJ, Koh DM. Computed diffusion-weighted MR imaging may improve tumor detection. Radiology. 2011;261(2):573–81.
28. Maas MC, Futterer JJ, Scheenen TW. Quantitative evaluation of computed high B value diffusion-weighted magnetic resonance imaging of the prostate. Invest Radiol. 2013;48(11):779–86.
29. Rosenkrantz AB, Chandarana H, Hindman N, Deng FM, Babb JS, Taneja SS, et al. Computed diffusion-weighted imaging of the prostate at 3 T: impact on image quality and tumour detection. Eur Radiol. 2013;23(11):3170–7.
30. Bittencourt LK, Attenberger UI, Lima D, Strecker R, de Oliveira A, Schoenberg SO, et al. Feasibility study of computed vs measured high b-value (1400 s/mm(2)) diffusion-weighted MR images of the prostate. World J Radiol. 2014;6(6):374–80.
31. Gibbs P, Liney GP, Pickles MD, Zelhof B, Rodrigues G, Turnbull LW. Correlation of ADC and T2 measurements with cell density in prostate cancer at 3.0 Tesla. Invest Radiol. 2009;44(9):572–6.
32. Woodfield CA, Tung GA, Grand DJ, Pezzullo JA, Machan JT, Renzulli JF 2nd. Diffusion-weighted MRI of peripheral zone prostate cancer: comparison of tumor apparent diffusion coefficient with Gleason score and percentage of tumor on core biopsy. AJR Am J Roentgenol. 2010;194(4):W316–22.
33. Verma S, Rajesh A, Morales H, Lemen L, Bills G, Delworth M, et al. Assessment of aggressiveness of prostate cancer: correlation of apparent diffusion coefficient with histologic grade after radical prostatectomy. AJR Am J Roentgenol. 2011;196(2):374–81.
34. Turkbey B, Shah VP, Pang Y, Bernardo M, Xu S, Kruecker J, et al. Is apparent diffusion coefficient associated with clinical risk scores for prostate cancers that are visible on 3-T MR images? Radiology. 2011;258(2):488–95.
35. • Bittencourt LK, Barentsz JO, de Miranda LC, Gasparetto EL. Prostate MRI: diffusion-weighted imaging at 1.5T correlates better with prostatectomy Gleason Grades than TRUS-guided biopsies in peripheral zone tumours. Eur Radiol. 2012;22(2):468–75. *This study reports a significant inverse correlation between the ADC value s of suspious lesions on prostate MRI and the Gleason score determined at radical prostatectomy. Of note, the Gleason score determined at prostatectomy showed a significantly stronger association with ADC values than with the Gleason score determined at biopsy.*
36. Lebovici A, Sfrangeu SA, Feier D, Caraiani C, Lucan C, Suciu M, et al. Evaluation of the normal-to-diseased apparent diffusion coefficient ratio as an indicator of prostate cancer aggressiveness. BMC Med Imaging. 2014;14(1):15.
37. Litjens GJ, Hambrock T, Hulsbergen-van de Kaa C, Barentsz JO, Huisman HJ. Interpatient variation in normal peripheral zone apparent diffusion coefficient: effect on the prediction of prostate cancer aggressiveness. Radiology. 2012;265(1):260–6.
38. Rosenkrantz AB, Triolo MJ, Melamed J, Rusinek H, Taneja SS, Deng FM. Whole-lesion apparent diffusion coefficient metrics as a marker of percentage Gleason 4 component within Gleason 7 prostate cancer at radical prostatectomy. J Magn Reson Imaging. 2014. doi:10.1002/jmri.24598.
39. Donati OF, Mazaheri Y, Afaq A, Vargas HA, Zheng J, Moskowitz CS, et al. Prostate cancer aggressiveness: assessment with whole-lesion histogram analysis of the apparent diffusion coefficient. Radiology. 2014;271(1):143–52.
40. Jensen JH, Helpern JA, Ramani A, Lu H, Kaczynski K. Diffusional kurtosis imaging: the quantification of non-gaussian water diffusion by means of magnetic resonance imaging. Magn Reson Med. 2005;53(6):1432–40.
41. Suo S, Chen X, Wu L, Zhang X, Yao Q, Fan Y, et al. Non-Gaussian water diffusion kurtosis imaging of prostate cancer. Magn Reson Imaging. 2014;32(5):421–7.
42. Rosenkrantz AB, Sigmund EE, Johnson G, Babb JS, Mussi TC, Melamed J, et al. Prostate cancer: feasibility and preliminary experience of a diffusional kurtosis model for detection and assessment of aggressiveness of peripheral zone cancer. Radiology. 2012;264(1):126–35.
43. Quentin M, Pentang G, Schimmoller L, Kott O, Muller-Lutz A, Blondin D, et al. Feasibility of diffusional kurtosis tensor imaging in prostate MRI for the assessment of prostate cancer: preliminary results. Magn Reson Imaging. 2014. doi:10.1016/j.mri.2014.04.005.
44. Yacoub JH, Verma S, Moulton JS, Eggener S, Aytekin O. Imaging-guided prostate biopsy: conventional and emerging techniques. Radiographics. 2012;32(3):819–37.
45. Van der Kwast TH, Roobol MJ. Defining the threshold for significant versus insignificant prostate cancer. Nat Rev Urol. 2013;10(8):473–82.
46. Noguchi M, Stamey TA, McNeal JE, Yemoto CM. Relationship between systematic biopsies and histological features of 222 radical prostatectomy specimens: lack of prediction of tumor significance for men with nonpalpable prostate cancer. J Urol. 2001;166(1):104–9 discussion 9-10.

47. Mufarrij P, Sankin A, Godoy G, Lepor H. Pathologic outcomes of candidates for active surveillance undergoing radical prostatectomy. Urology. 2010;76(3):689–92.
48. Rabbani F, Stroumbakis N, Kava BR, Cookson MS, Fair WR. Incidence and clinical significance of false-negative sextant prostate biopsies. J Urol. 1998;159(4):1247–50.
49. Rajinikanth A, Manoharan M, Soloway CT, Civantos FJ, Soloway MS. Trends in Gleason score: concordance between biopsy and prostatectomy over 15 years. Urology. 2008;72(1):177–82.
50. Onik G, Miessau M, Bostwick DG. Three-dimensional prostate mapping biopsy has a potentially significant impact on prostate cancer management. J Clin Oncol. 2009;27(26):4321–6.
51. • Haffner J, Lemaitre L, Puech P, Haber GP, Leroy X, Jones JS et al. Role of magnetic resonance imaging before initial biopsy: comparison of magnetic resonance imaging-targeted and systematic biopsy for significant prostate cancer detection. BJU Int. 2011;108(8 Pt 2):E171–8. *This article represents one of the first works to demonstrate the potential value of MRI and MRI-targeted biopsy in a large cohort of biopsy-naïve men. Specifically, in 555 men undergoing prebiopsy MRI, MRI-targeted cores detected more significant cancer and less insignificant cancer than non-targeted systematic cores*.
52. Overduin CG, Futterer JJ, Barentsz JO. MRI-guided biopsy for prostate cancer detection: a systematic review of current clinical results. Curr Urol Rep. 2013;14(3):209–13.
53. Siddiqui MM, Rais-Bahrami S, Truong H, Stamatakis L, Vourganti S, Nix J, et al. Magnetic resonance imaging/ultrasound-fusion biopsy significantly upgrades prostate cancer versus systematic 12-core transrectal ultrasound biopsy. Eur Urol. 2013;64(5):713–9.
54. Pinto PA, Chung PH, Rastinehad AR, Baccala AA Jr, Kruecker J, Benjamin CJ, et al. Magnetic resonance imaging/ultrasound fusion guided prostate biopsy improves cancer detection following transrectal ultrasound biopsy and correlates with multiparametric magnetic resonance imaging. J Urol. 2011;186(4):1281–5.
55. Maxeiner A, Fischer T, Stephan C, Cash H, Slowinski T, Kilic E, et al. Real-time MRI/US fusion-guided biopsy improves detection rates of prostate cancer in pre-biopsied patients. Aktuelle Urol. 2014;45(3):197.
56. Rubin R, Siddiqui MM, George A, Walton-Diaz A, Rais-Bahrami S, Su D, et al. MP53-03 the efficiency of MRI/US fusion targeted prostate biopsies in finding clinically significant prostate cancer compared to standard template biopsy. J Urol. 2014;191(4S):e589.
57. Le JD, Stephenson S, Brugger M, Lu DY, Lieu P, Sonn GA, et al. MRI-ultrasound fusion biopsy for prediction of final prostate pathology. J Urol. 2014. doi:10.1016/j.juro.2014.04.094.
58. Rosa MR, Milot L, Sugar L, Vesprini D, Chung H, Loblaw A, et al. A prospective comparison of MRI-US fused targeted biopsy versus systemic ultrasound-guided biopsy for detecting clinically significant prostate cancer in patients on active surveillance. J Magn Reson Imaging. 2014. doi:10.1002/jmri.24710.
59. Moore CM, Robertson NL, Arsanious N, Middleton T, Villers A, Klotz L, et al. Image-guided prostate biopsy using magnetic resonance imaging-derived targets: a systematic review. Eur Urol. 2013;63(1):125–40.
60. • Vourganti S, Rastinehad A, Yerram NK, Nix J, Volkin D, Hoang A et al. Multiparametric magnetic resonance imaging and ultrasound fusion biopsy detect prostate cancer in patients with prior negative transrectal ultrasound biopsies. J Urol. 2012;188(6):2152–7. *This study demonstrates the potential role of MRI-ultrasound fusion biopsy in a cohort of 195 men with prior negative prostate biopsies. MRI-utrasound fusion cores resulted in tumor upgrading in 38.9 % of patients in comparison with standard systematic cores*.
61. Sonn GA, Chang E, Natarajan S, Margolis DJ, Macairan M, Lieu P, et al. Value of targeted prostate biopsy using magnetic resonance-ultrasound fusion in men with prior negative biopsy and elevated prostate-specific antigen. Eur Urol. 2014;65(4):809–15.
62. Cornud F, Brolis L, Delongchamps NB, Portalez D, Malavaud B, Renard-Penna R, et al. TRUS-MRI image registration: a paradigm shift in the diagnosis of significant prostate cancer. Abdom Imaging. 2013;38(6):1447–63.
63. Marks L, Young S, Natarajan S. MRI-ultrasound fusion for guidance of targeted prostate biopsy. Curr Opin Urol. 2013;23(1):43–50.
64. Wysock JS, Rosenkrantz AB, Huang WC, Stifelman MD, Lepor H, Deng FM, et al. A prospective, blinded comparison of magnetic resonance (MR) imaging-ultrasound fusion and visual estimation in the performance of MR-targeted prostate biopsy: the PROFUS trial. Eur Urol. 2013. doi:10.1016/j.eururo.2013.10.048.
65. van de Ven WJ, Hulsbergen-van de Kaa CA, Hambrock T, Barentsz JO, Huisman HJ. Simulated required accuracy of image registration tools for targeting high-grade cancer components with prostate biopsies. Eur Radiol. 2013;23(5):1401–7.
66. Martin PR, Cool DW, Romagnoli C, Fenster A, Ward AD. Magnetic resonance imaging-targeted, 3D transrectal ultrasound-guided fusion biopsy for prostate cancer: quantifying the impact of needle delivery error on diagnosis. Med Phys. 2014;41(7):073504.